Preprints.org

Article

Not peer-reviewed version

Rupestonic Acid Derivative YZH-106 Promotes Lysosomal Degradation of HBV L- and M-HBsAg via Direct Interaction with PreS2 Domain

Lanlan Liu , Haoyu Wang , Lulu Liu , Fang Cheng , Haji Akber Aisa , Changfei Li * , Songdong Meng *

Posted Date: 7 May 2024

doi: 10.20944/preprints202405.0371.v1

Keywords: YZH-106; HBV; HBsAg; degradation

doi:10.20944/preprints202405.0371.v1

Article

Rupestonic Acid Derivative YZH-106 Promotes Lysosomal Degradation of HBV L- and M-HBsAg via Direct Interaction With PreS2 Domain

Lanlan Liu [1,†], Haoyu Wang [1,2,†], Lulu Liu [1], Fang Cheng [1,2], Haji Akber Aisa [3], Changfei Li [1,*] and Songdong Meng [1,2,*]

1 Key Laboratory of Pathogenic Microbiology and Immunology, Institute of Microbiology, Chinese Academy of Sciences, Beijing, China
2 University of Chinese Academy of Science, Beijing, China
3 State Key Laboratory Basis of Xinjiang Indigenous Medicinal Plants Resource Utilization, Xinjiang Technical Institute of Physics and Chemistry, Chinese Academy of Sciences, Xinjiang, China
* Correspondence: lichangfei2006@163.com (C.L.); mengsd@im.ac.cn (S.M.)
† These authors contribute equally to this work.

Abstract: Hepatitis B surface antigen (HBsAg) is not only the biomarker of hepatitis B virus (HBV) infection and expression activity in hepatocytes, but also contributes to viral specific T cell exhaustion and HBV persistent infection. Therefore, anti-HBV therapies targeting HBsAg to achieve HBsAg loss are key approaches for HBV functional cure. In this study, we found that YZH-106, a rupestonic acid derivative, inhibited HBsAg secretion and viral replication. Further investigation demonstrated that YZH-106 promoted the lysosomal degradation of viral L- and M-HBs proteins. Mechanistic study by Biacore and docking analysis revealed that YZH-106 bound directly to PreS2 domain of L- and M-HBsAg, thereby blocking their entry to the endoplasmic reticulum (ER) and promoting their degradation in cytoplasm. Our work thereby provide basis for design of novel compound therapy to target HBsAg against HBV infection.

Keywords: YZH-106; HBV; HBsAg; degradation

Introduction

Hepatitis B virus (HBV) infection affects about 250 million patients worldwide and poses a major global health problem. HBV infectious virions have an icosahedral nucleocapsid composed of hepatitis B core protein (HBc), viral polymerase (Pol), and viral genome DNA. The nucleocapsid is surrounded by viral envelope containing large, middle and small viral surface antigens (HBs) [1]. Hepatitis B surface antigen (HBsAg) proteins differ in their N-terminus but share a common S domain on their C-terminus. The middle surface antigen (M-HBsAg) contains an additional region, the preS2 region, at the N-terminus of the small surface protein (S-HBsAg), and the large surface antigen (L-HBsAg) carries the PreS2 and PreS1 domains at the N-terminus of S-HBsAg [2]. Under HBV infection HBsAg production and secretory pathway and the viral replication pathway are largely distinctive processes within the hepatocyte[3]. After translation from two HBV sub-genomic mRNA transcripts in cytoplasm, the small, middle and large surface proteins assemble in the endoplasmic reticulum (ER) to generate noninfectious sub-viral particles (SVPs) with either a spherical or a long filamentous form. The SVPs are secreted via the Golgi pathway or multivesicular body-associated endosomal sorting complex required for transport (ESCRT) machinery. Meanwhile, viral genome-containing nucleocapsids are assembled with the three surface proteins to form infectious virions, and then are secreted by ESCRT pathway.

Chronic HBV infection (CHB) is characterized by large amounts of complete virus, as well as noninfectious envelope particles that are secreted in serum at levels far in excess of mature virions and are believed to play a key role as a decoy for antiviral immunity. It has been reported that monocytes, dendritic cells, nature killer cells and nature killer T cells were inhibited by direct

 doi:10.20944/preprints202405.0371.v1

interaction with HBsAg. Large numbers of HBsAg could also cause exhaustion of virus-specific cytotoxic T lymphocytes (CTLs) and helper T (Th) cells. Therefore, HBsAg acts not only as the biomarker of HBV infection and expression activity in hepatocytes, but also majorly contribute to HBV persistent infection [4–6].

Recent studies for CHB therapy have been focused on establishing a functional cure, defined as sustainable HBsAg seroclearance (HBsAg loss), undetectable serum HBV DNA levels, with or without HBsAg antibody seroconversion [7-9]. Anti-viral therapies targeting HBsAg include RNA interference (RNAi), anti-sense oligonucleotide (ASO) and nucleic acid polymers selectively suppressing SVPs assembly and/or secretion [10]. RNAi-based therapy against CHB has been studied in Phase II clinical trial, and it has demonstrated that HBsAg can be effectively reduced by treatment and thus hold promise for HBsAg loss [11,12].

Artemisia rupestris L, is a traditional herb with antitumor, detoxification, anti-antiviral, antibacterial, and anti-inflammatory activities [13,14]. Rupestonic acid could be extracted from Artemisia rupestris L. and more than 200 rupestonic acid derivatives have been synthesized by researchers. Compound YZH-106, a member of rupestonic acid derivatives with phenyl isoxazole modified to its carboxyl group, displayed activities against a broad-spectrum of influenza viruses (IAV) including drug-resistant IAV strains [15,16]. In this study, we provide experimental evidence that YZH-106 could bind directly to PreS2 domain of L and M-HBsAg, which blocked L and M-HBsAg entry to ER and promoted their degradation by lysosome. Therefore, our results reveal a novel mechanism by which HBsAg was targeted for degradation. The results may offer a novel therapeutic strategy for the HBV infection treatment.

Material and Methods

2.1. Reagents and Antibodies

The following reagents and antibodies were obtained as indicated: YZH106 with more than 98% purity was originally provided by Xinjiang Technic Institute of Physics and Chemistry, Chinese Academy of Sciences. HBsAg antibody, PreS2 antibody, Calnexin antibody, Lamp1 antibody, and ubiquitin antibody were purchased from Abcam. GAPDH antibody and HRP-conjugated secondary antibody were obtained from Beijing Zhong Shan Golden Bridge Biotechnology. MG132 was from Selleck Chemicals LLC; and the ECL Plus chemiluminescence system was from Beyotime Biotechnology.

2.2. Cell Culture and Transfection

The human hepatoma cell line Huh-7 was obtained from the ATCC (Manassas, VA), and HepG2.2.1.5, which has been stably transformed with 1.3 copies of the HBV genome, was maintained in the lab. Cells were cultured in Dulbecco's modified Eagle medium (DMEM, Gibco) supplemented with 10% FBS (Invitrogen), 100 μg/ml streptomycin and 100 IU/ml penicillin at 37°C in a 5% CO2 incubator. For HepG2.2.1.5 culture, 380 μg/ml G418 (Invitrogen) was added to DMEM.

Huh-7 cells were washed twice with Opti-MEM (Invitrogen), and transfected with pHBV1.3 plasmid using Lipofectamine 2000 reagent (Invitrogen).

2.3. Detection of HBsAg and HBeAg

The expression levels of HBsAg and HBeAg in cell supernatants were determined using enzyme-linked immunosorbent assay (ELISA) kits (Shanghai Kehua Bio-engineering Co., Ltd.) according to the manufacturer's instructions. All experiments were conducted in triplicate.

2.4. Cell Proliferation Assay

Cell proliferation was carried out using the Cell-Counting Kit (CCK)-8 (Dojindo, Kumamoto, Japan) as described [17]

2.5. RT-PCR Analysis

Viral DNA copy numbers in culture medium was detected using an HBV nucleic acid RT-PCR kit (Hangzhou Bioer Technology) at 24h after addition of YZH-106. Total RNA was extracted from cells using TRIzol (Invitrogen). First-strand cDNA was synthesized with an oligo(dT)-adaptor primer and AMV reverse transcriptase (Takara). PCR primers are listed in Table 1, with the β-actin gene serving as an internal control. Amplification products were analyzed by 1.5% agarose gel electrophoresis.

Table 1. Name and sequence of qRT-PCR primers used in this study.

Name	Sequence 5′-3′
pgRNA forward	TCTTGCCTTACTTTTGGAAG
pgRNA reverse	AGTTCTTCTTCTAGGGGACC
total RNA forward	CTCCCCGTCTGTGCCTTCTC
total RNA reverse	TCGGTCGTTGACATTGCTGA
PreC RNA forward	GAGTGTGGATTCGCACTCC
PreC RNA reverse	GAGGCGAGGGAGTTCTTCT
HBsAg RNA forward	CACATCAGGATTCCTAGGACC
HBsAg RNA reverse	GGTGAGTGATTGGAGGTTG
PreS2 RNA forward	CCACCATGCAGTGGAACTC
PreS2 RNA reverse	TGTGTTCTCCATGTTCGGTG

2.6. Immunoprecipitation (IP) and Western Blot Analysis

After treatment with YZH-106, cells were harvested and lysed using ice-cold NP40 cell lysis buffer. Equal amounts of total proteins were incubated with 2 μL primary antibodies or IgG as a control for 2~3 h at 4 ℃. Then, protein A&G Sepharose beads (Santa Cruz Biotech) were added and incubated with the cell lysates overnight at 4℃. The beads were washed four times with cell lysis buffer and resuspended in 5X SDS-PAGE loading buffer. The proteins were separated by SDS-PAGE and analyzed by Western blot.

2.7. The Endoplasmic Reticulum and Cytoplasm Components Isolation

Isolation of the ER proteins was performed by an ER protein extraction kit (BB-31454, BestBio), and cytoplasmic proteins were extracted from cells using special lysis buffer (BB-36021, BestBio). In brief, cells were harvested after centrifugation at 500×g for 5 min, and washed with cold PBS. For ER protein extraction, a Dounce homogenizer was used to fully homogenize cells after Solution A was added. After centrifugation at 1000×g for 10 min at 4 °C, the supernatant was collected, and centrifuged at 12,000×g for another 10 min at 4 °C. The pellet was then resuspended in Solution B and centrifuged at 45,000×g for 45 min at 4 °C. Finally, the pellet was resuspended in Solution C and the ER proteins were acquired. For isolating cytoplasmic protein, cold special lysis buffer was added to the cell pellet. After the pellet was mixed by vortex, and kept on ice for 30 min, the cell lysate was centrifuged at 1,200×g for 5 min at 4 °C. The supernatant was collected to obtain the cytosolic fraction.

2.8. Immunofluorescence (IF)

After cells were treated with YZH-106 for 24 h, they were fixed with 4% paraformaldehyde and incubated with 5% BSA. Then the cells were incubated with primary antibody and TRITC or FITC-conjugated secondary antibody. Images were obtained on a Leica TCS SP8 confocal laser-scanning microscope (Leica Microsystems, Germany).

2.9. Expression and Purification of Protein

The optimized coding sequence of the HBV PreS1-PreS2 (GenBank: CCH63721.1) was cloned into the pET-28a (+)-sumo expression vector and the resulting vector was named pET-28a-PreS. This

 doi:10.20944/preprints202405.0371.v1

vector includes an N-terminal 6×His tag and a C-terminal SUMO tag. PreS1-PreS2 protein was expressed in E. coli BL21(DE3) pLysS (Invitrogen, Madison, WI, USA) with induction of IPTG. Bacteria was lysed by sonication and supernatant was acquired after centrifugation. Protein was then purified sequentially through a His-trap HP column (Cytiva), and a HiTrap Q HP column (Cytiva). The purified protein was assessed by 15% Coomassie stained SDS-PAGE.

2.10. Surface Plasmon Resonance (SPR) Assay

The affinity between PreS1-PreS2 protein and YZH-106 was measured using a Biacore 8K system. PreS1-PreS2 protein was immobilized on CM5 chips (Cytiva) at a concentration of 1 mg/mL, and serial dilutions of YZH-106 were added.

2.11. Molecular Docking

The three-dimensional structures of Pre-S1 and PreS1-PreS2 proteins were predicted using AlphaFold following standard protocols. Molecular docking of YZH-106 with these proteins was performed with MOEDOCK (MOE), utilizing the AMBER10: EHT force field and the R-field implicit solvation model for optimization. Ligand structures were obtained from PubChem and prepared using MOE's energy minimization. Binding sites were identified with MOE's 'Site Finder', focusing on specific residues for each protein. The most likely binding modes were determined based on the lowest binding free energy, visualized using PyMOL.

2.12. Statistical Analysis

Data were expressed as percentage, mean ± SD. Comparisons between two groups were analyzed by the student t test. $P < 0.05$ was considered statistically significant.

Results

Rupestonic Acid Derivative YZH-106 Suppresses HBsAg Secretion

In this study, we first examined whether the rupestonic acid YZH-106 could suppress HBV expression and replication. As seen in Figure 1A and 1B, HBsAg and HBeAg secretion in HepG2.2.15 cells with stable transfection HBV expression were reduced by YZH-106 treatment in a dose dependent manner. Moreover, YZH-106 caused more decrease of HBsAg than HBeAg. To determine if the decrease of HBV replication caused by YZH-106 was related to inhibition of cell proliferation induced by YZH-106. CCK-8 analysis was performed to examine the effect of YZH-106 on proliferation of HepG2.2.15 cells. As illustrated in Figure 1C, treatment with YZH-106 at concentrations of 4 μM or less had no significant effect on HepG2.2.15 cell proliferation by CCK8 analysis, excluding the possibility that YZH-106 affects HBV expression through inhibition of cell growth. Thus, 3 μM YZH-106 was selected to perform the following experiments.

As shown in Figure 1 D, treatment with 3 μM YZH-106 caused approximately 58% and 48% reductions in levels of HBsAg and HBV-DNA in the cell supernatant (both $P<0.001$). In contrast, no obvious changes in HBV mRNA levels were observed in YZH-106-treated cells (Figure 1E), indicating that YZH-106 affected HBsAg levels not through inhibition of HBV transcription.

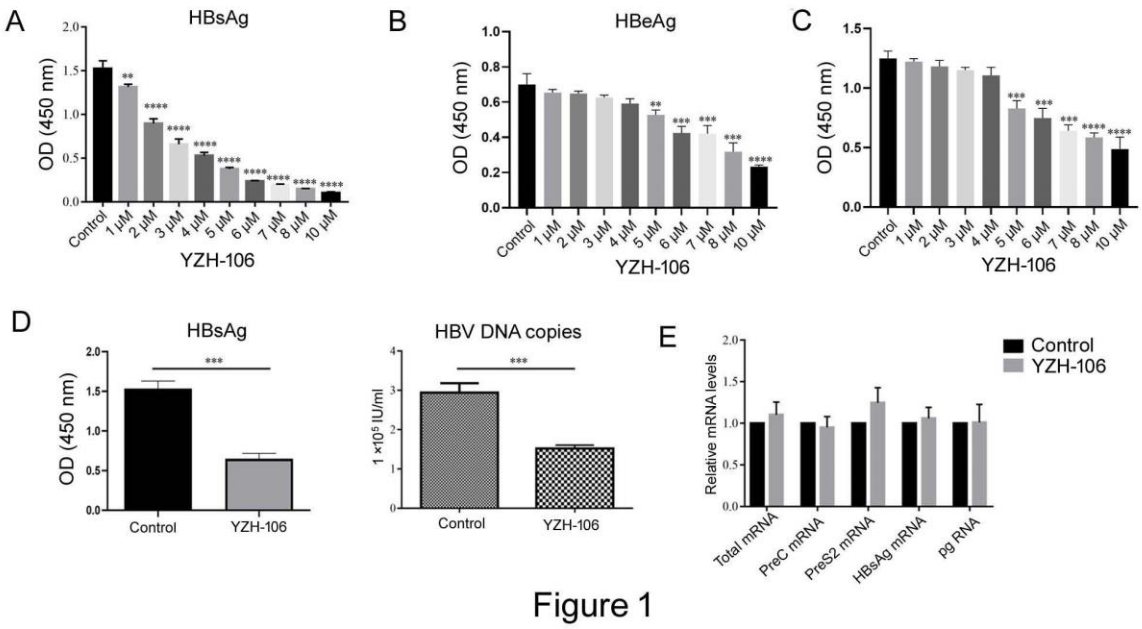

Figure 1. YZH-106 inhibited HBsAg secretion and decreased L-HBsAg and M-HBsAg protein levels. (A-C) HepG2.2.1.5 cells were treated with the indicated doses of YZH-106 or DMSO as a control. At 72 h after treatment, levels of HBsAg (A) or HBeAg (B) in the supernatant was measured by ELISA and cell proliferation was detected by CCK-8 assay (C). (D, E) HepG2.2.1.5 cells were treated with the 3 μM YZH-106 or DMSO as a control. At 24 h after treatment, HBsAg or HBV DNA copies in the supernatant (D) or HBV mRNA levels in cells (E) were quantified by ELISA or real-time PCR respectively. GAPDH was used as an internal control. Data are presented as the means ± SD from three independent experiments. **P < 0.01, ***P<0.001 and ****P<0.0001 compared to control.

YZH-106 Promotes the Lysosomal Degradation of L- and M-HBs Protein

To investigate the underlying mechanism for YZH-106-mediated inhibition of HBsAg secretion, levels of HBV envelope proteins L/M/S-HBs were determined. Western-blot analysis revealed that L- and M-HBsAg but not S-HBsAg levels in HepG2.2.15 cells or Huh-7 cells transfected with pHBV1.3 were reduced under YZH-106 treatment compared to control (Figure 2A). As YZH-106 inhibited HBsAg production not via transcriptional regulation, the stability of HBV envelope proteins was then analyzed. As seen in Figure 2B, YZH-106 caused a dramatic reduction in the protein stability of L- and M-HBs in the presence of protein synthesis inhibitor cycloheximide (CHX). Compared to control no obvious change at levels of HBs ubiquitination was observed in YZH-106 treated cells (Figure 2C). In addition, YZH-106-induced reduction of L- and M-HBs could largely be restored by treatment with the lysosomal protease inhibitors E64d and Pepstatin A (Figure 2D). Fluorescence microscopy was further used to analyze the influence of YZH-106 on co-localization of PreS2 and lamp1, the marker of lysosome. As illustrated in Figure 2E, co-localization of PreS2 and lamp1 was significantly increased upon treatment with YZH-106. All together, these data indicate that YZH-106 mediated downregulation of L- and M-HBs mainly through lysosomal degradation.

 doi:10.20944/preprints202405.0371.v1

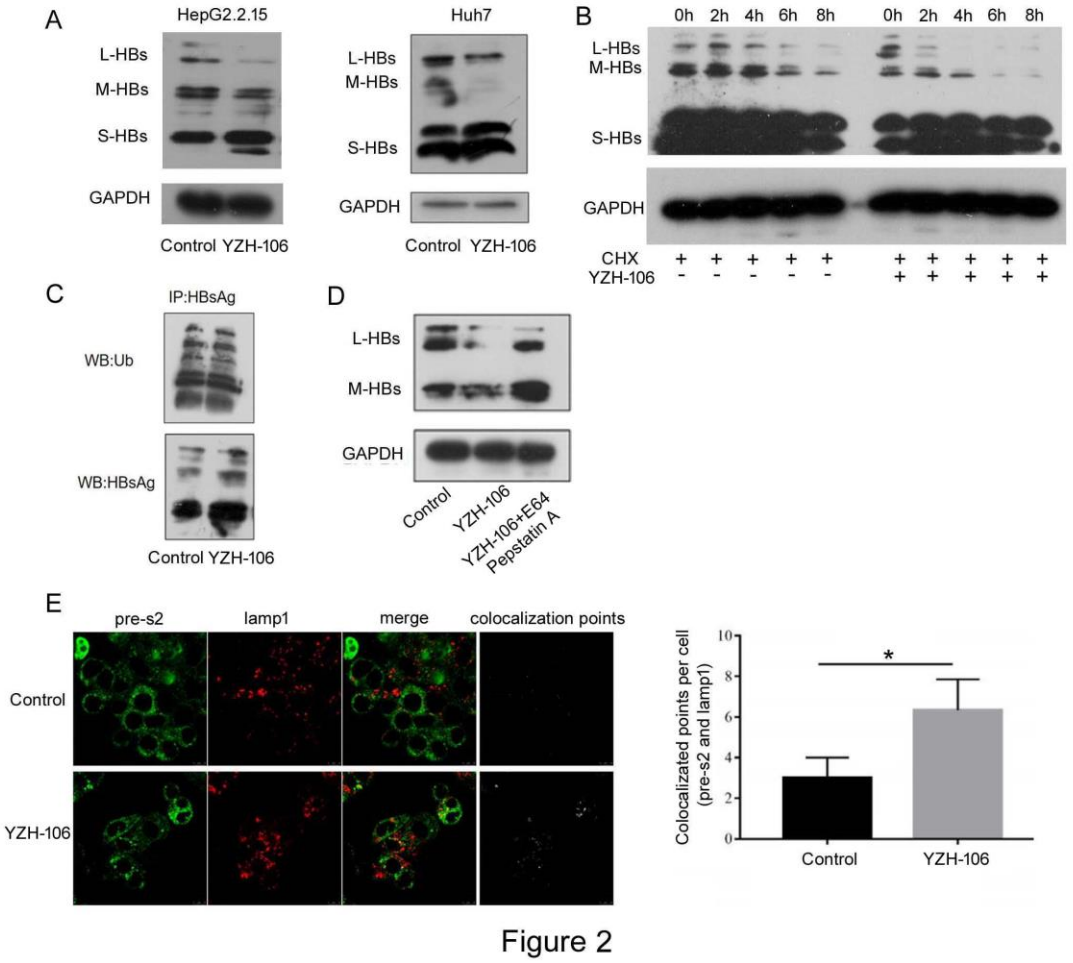

Figure 2. YZH-106 induced lysosomal degradation of L- and M-HBs protein. (A) HepG2.2.1.5 or Huh-7 cells transfected with 1.3 copies of HBV were treated with 3 μM YZH-106 or DMSO as a control, respectively. At 24 h after treatment, L-HBs, M-HBs and S-HBs protein levels were detected by Western blotting. (B) HepG2.2.1.5 cells in the presence of the translation inhibitor CHX were treated with 3 μM YZH-106 or DMSO as a control for the indicated times. Then L-, M- and S-HBs protein levels were detected by Western blotting. (C) HepG2.2.1.5 cells were treated with 3 μM YZH-106 for 24 h and exposed to 20 μM MG132 for 6 h before lysis. HBs protein was immunoprecipitated and subjected to immunoblot with an antibody specific to ubiquitin. (D) HepG2.2.1.5 cells were treated with 3 μM YZH-106 alone for 24 h or together with E64d and Pepstatin A. L- and M-HBs proteins were analysed by western blotting. (E) Immunofluorescence staining was performed to analyze the co-localization of PreS2 (Green) andlamp1 (red) in YZH-106 treated HepG2.2.1.5 cells. The colocalization points were computed by Image J. Data are presented as the means ± SD from three independent experiments. * $P< 0.05$ compared to control. The experiments were performed twice with similar results.

L- and M-HBs Levels in the ER but Not in Cytoplasm Are Obviously Reduced Upon YZH-106 Treatment

After HBs proteins are translated in cytoplasm, they quickly translocate to and accumulate in the ER and form agglomerates through covalent disulfide bridges with different cysteines in their S domain, which then are secreted from the cell as new infectious virions as well as noninfectious envelope particles [17]. We then investigated at which step that YZH-106 may affect HBsAg secretion. The cytoplasmic and ER components in HepG2.2.15 cells under YZH-106 treatment for 48h were isolated and HBs proteins were examined by Western blot analysis. As demonstrated in Figure 3A, treatment with YZH-106 led to decreased L- and M-HBs but not S-HBs protein levels in ER compared to control. Whereas there was almost no change of L and M-HBs protein levels in cytoplasm upon

Preprints.org (www.preprints.org) | NOT PEER-REVIEWED | Posted: 7 May 2024 doi:10.20944/preprints202405.0371.v1

treatment with YZH-106. The co-localization of PreS2 and the ER marker calnexin or cytoplasm marker HSP70 was further evaluated by using fluorescence microscope. As shown in Figure 3B and 3C, co-localization of PreS2 and calnexin but not HSP70 was significantly declined by YZH-106. Collectively, these data suggest that YZH-106 suppressed L and M-HBs protein entry into ER.

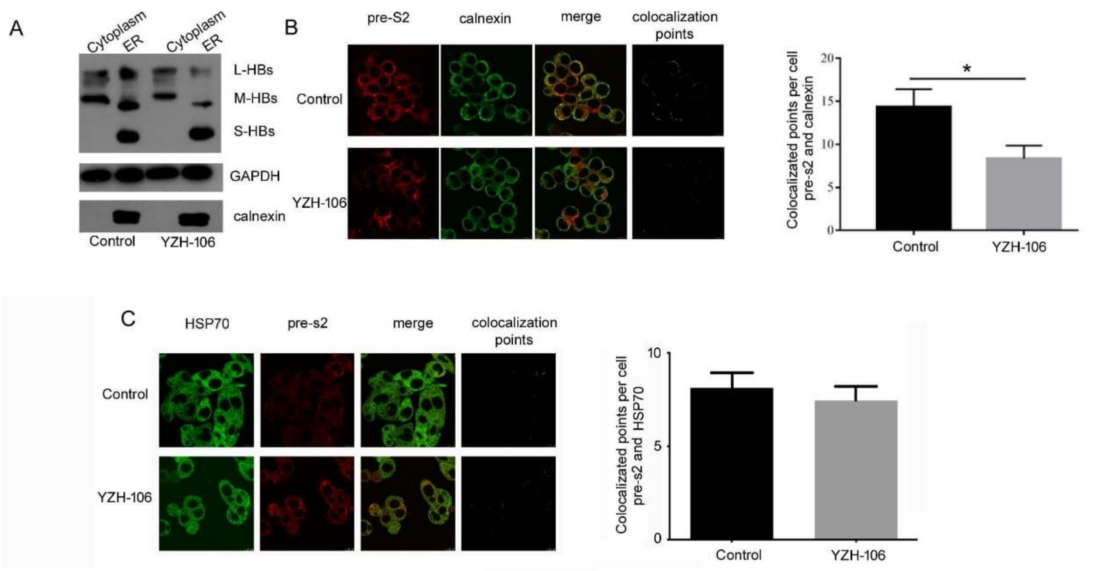

Figure 3

Figure 3. YZH-106 treatment reduced L- and M-HBs protein levels in the ER. (A) The cytoplasmic and ER components in HepG2.2.15 cells treated with YZH-106 were isolated and L-, M- and S-HBs proteins were examined by western blotting analysis. (B, C) Immunofluorescence was performed to analyze the co-localization of PreS2 (Red) and ER marker Calnexin (Green) (B) or cytoplasmic marker HSP70 (Green) (C) in YZH-106 treated HepG2.2.1.5 cells, and the colocalization points were computed by Image J. Data are presented as the means ± SD from three independent experiments. * $P< 0.05$ compared to control.

YZH-106 Directly Binds to PreS2 Domain in L- and M-HBs Proteins

To explore the underlying basis for YZH-106-mediated blockage of L- and M-HBs entry into ER, we determined to test if YZH-106 could bind to L- or M-HBs protein. As YZH-106 was shown to induce degradation and block ER entry of L- and M-HBs but not S-HBs proteins, we speculated that YZH-106 may interact with the shared PreS2 domain of L- and M-HBs. His-tagged PreS1-PreS2 fusion protein expressed in *E. coli* was analyzed by Coomassie blue-staining and Western blotting (Figure 4A). The interaction of YZH-106 and PreS1-PreS2 protein was evaluated by a direct binding assay using the Biacore system. As illustrated in Figure 4B, YZH-106 bound to a PreS1-PreS2-conjugated sensor chip with fast kinetics. By using steady-state binding analysis, the binding affinity (Kd) was calculated at 279 μM.

Finally, molecular docking was performed with ZDOCK Server (version 3.0.2) to analyze the intra-molecular interactions between YZH-106 and PreS1-PreS2 or PreS1 protein. PreS1-PreS2 or PreS1 protein structures were firstly predicted using AlphaFold software, then proteins were separately docked and modeled in complex with YZH-106. It was found that the potential binding sites for YZH-106 and PreS1-PreS2 protein span from Arg102 to Ser152 adjacent or within PreS2, while no binding sites were observed within PreS1 domain (Figure 4C, Figure S1). Furthermore, MOE-Dock simulation study was carried out to determine the binding affinity of the compound with proteins. The docking score was summarized in Table 2. The more negative the docking score, the better the binding affinity between the compound with proteins. The docking score between YZH-106 compound with PreS1 was -2.89 kcal/mol, and the docking score between YZH-106 with PreS1-PreS2 protein was -6.77 kcal/mol, indicating a relatively much stronger affinity between YZH-106 and

 doi:10.20944/preprints202405.0371.v1

PreS1-PreS2.Together, these results validate that YZH-106 binds directly to PreS2 domain of L- and M-HBs protein, which may inhibit their translocation to ER.

Table 2. Docking scores.

Ligand	Receptor	Binding energy (kcal/mol)
Compound	pre-s1	-2.89
Compound	pre-s1/pre-s2	-6.77

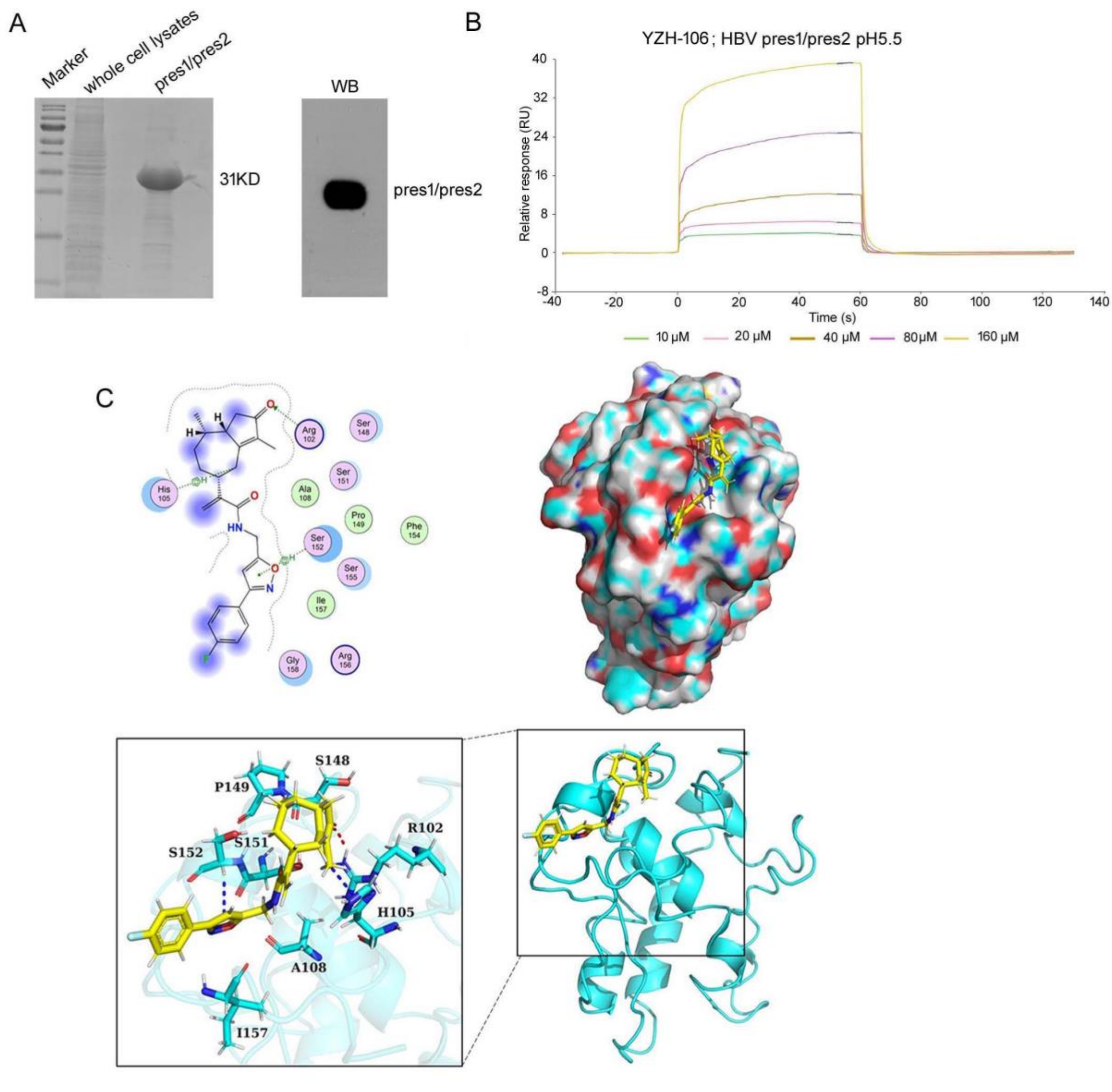

Figure 4

Figure 4. YZH-106 binds to PreS2 domain. (A)Expression and purification of His-tagged PreS1-PreS2 fusion protein in *E. coli*. The purified protein was subjected to SDS-PAGE and stained with Coomassie Blue or immunobloted with an anti-PreS2 Ab. (B) Interaction of YZH-106 and PreS1-PreS2 fusion protein was evaluated by a direct binding assay using the Biacore system. (C) YZH-106 docking model with PreS1-PreS2 fusion protein. Top-left: the 2D binding mode of YZH-106 and PreS1-PreS2. Top-right: the surface binding mode of YZH-106 and PreS1-PreS2. Bottom: the 3D binding mode of YZH-106 and PreS1-PreS2.YZH-106 and PreS1-PreS2 residues are colored in yellow and cyan respectively. The residue Arg102 adjacent or within PreS2 forms a hydrogen bond with YZH-106. Additionally, residues His105 and Ser152 each engage in two H-Pi conjugation interactions with YZH-106,

 doi:10.20944/preprints202405.0371.v1

respectively. The interaction amino acids between YZH-106 and PreS1-PreS2 are shown as blue or red sticks, and non-carbon atoms are colored according to their chemical identity (C, cyan or yellow; O, red; N, blue; H, white).

Discussion

Chronic HBV infection causes severe liver disease including cirrhosis and liver failure and increases risk of hepatocellular carcinoma occurrence. Current antiviral treatments for CHB include PEG-interferon and nucleos(t)ide analogues (NAs). However, both agents have limited therapeutic efficacy in HBsAg loss [9,18]. Our data demonstrated that a rupestonic acid derivative YZH-106 efficiently suppressed HBsAg secretion in HBV stably expressed HepG2.2.15 cells. Further investigation revealed that the protein levels of the surface proteins L-HBs and M-HBs were notably decreased via lysosomal degradation pathway under treatment with YZH-106. Biacore and docking analysis revealed that YZH-106 bound directly to PreS2 domain of L- and M-HBs, thereafter blocking their entry to ER and leading to their degradation (Figure 5). Our results offer a basis that YHZ-106 may be developed as a potential antiviral agent for HBV infection.

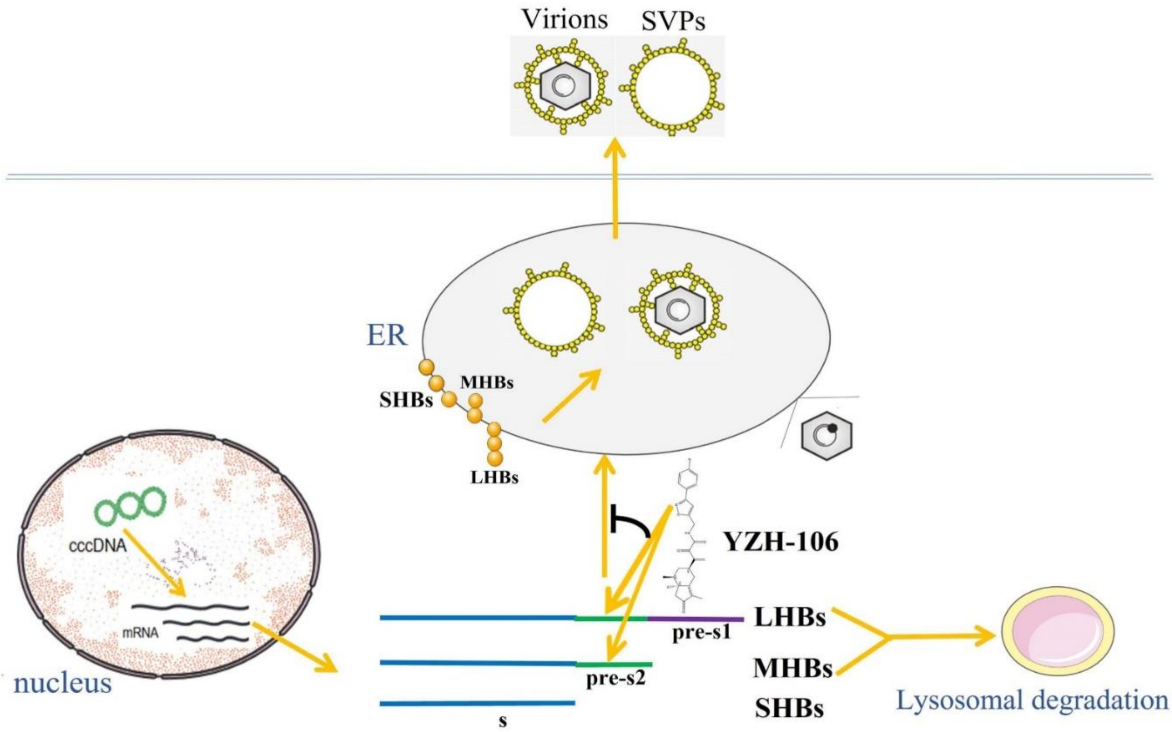

Figure 5

Figure 5. Schematic figure of YZH-106 mediated suppression of HBSAg. HBV L-HBs, M-HBs and SHBs proteins are translated in cytoplasm of infected cells. YZH-106 could bind to PreS2 domain of L-HBs and M-HBs protein, thereby inhibiting their entry to ER and promoting their lysosomal degradation. As a sequence, virial envelop assembly in the ER and secretion of HBsAg was decreased.

It has been reported that high level of HBsAg could lead to reduction of CD8+ T cell function and T cell exhaustion. In addition, HBsAg promotes the disease progression of CHB to liver cirrhosis and HCC [19,20]. Sustained HBsAg loss is defined as functional cure of CHB, which is related to improved clinical outcomes. Therefore, one of the primary goal of treatment outcomes for CHB is seroclearance and conversion of HBsAg [21,22]. Current anti-HBV agents inhibit HBsAg expression and secretion through various mechanisms such as suppression of HBV entry or HBsAg-release, siRNA, ASO, neutralization of HBsAg-release and inhibition of cccDNA [22–24]. It has been reported that siRNA and ASO based treatment strategies against CHB led to HBsAg decrease to very low

 doi:10.20944/preprints202405.0371.v1

levels, which resulted in reversion of T-cell anergy and reconstitution of the host immune response [11,25,26]. Up to now, natural compounds that exert their antiviral effects by direct binding to HBV surface proteins have not been reported. In our present study, we demonstrated that the rupestonic acid derivative YZH-106 could bind to PreS2 domain directly and cause degradation of L- and M-HBs proteins. The importance of a stable proportion of L-HBs, M-HBs, and S-HBs in the envelope of infectious as well as noninfectious viral particles is well established. Gerken et al. have demonstrated that during the transition from acute hepatitis B to HBsAg loss, the proportion of L-HBs and M-HBs in viral envelope decreases [27]. The roles of L-HBs in viral entry, morphogenesis, and output are critical. L-HBs-negative mutant strains were unable to form or secrete viral particles, suggesting that a reduction in L-HBs correlates with decrease of viral replication [28]. Meanwhile, M-HBs are shown to play a regulatory role in HBV replication, with their absence leading to reduced secretion of viral particles [29]. Pfefferkorn et al. also observed a decrease in L-HBs and M-HBs proportions prior to total HBsAg loss during NA and PEG-IFN treatment [30]. These studies suggest that inhibition of L- and M-HBs may lead to decreased HBV replication and eventually HBsAg loss.

In this study, we observed that reduction of L- and M-HBs levels induced by YZH-106 was largely restored by lysosomal enzyme inhibitors, indicating that YZH-106 mainly mediated lysosomal degradation of the viral surface proteins.

Protein degradation pathways are classified into proteasomal degradation and lysosomal degradation that can be further divided into three types: macroautophagy, microautophagy, and chaperone-mediated autophagy [31,32]. Interestingly, a previous study showed that inhibition of L-HBs chaperon HSC70 induced degradation of L-HBs with mutant PreS2 via the microautophagy-lysosomal pathway [33]. We consider that YZH-106 binds to PreS2 domain and might inhibit translocation of L- and M-HBs cross ER membrane topologically, thereby leading to their lysosomal degradation in cytoplasm.

In this study, we observed that YZH-106 has a medium binding affinity of -6.77 kcal/mol to PreS1-PreS2 protein. It will be helpful to optimize structure of YZH-106 to increase its affinity and specificity to PreS2 domain for the design of more potent anti-HBV drugs. In addition, we only assessed inhibitory activity of YZH-106 on HBsAg *in vitro*, and established the proof of principle that the rupestonic acid derivatives have the potential for the development of novel compound drugs targeting HBsAg. Experiments with HBV transgenic mice and AAV/HBV-infected mice models are needed to further evaluate HBsAg suppressing capability of YZH-106 and its optimized compounds and reversion of T cell tolerance to HBV.

Conclusion

In summary, we provide evidence that YZH-106 could directly bind to PreS2 domain of HBV L- and M-HBsAg, thereafter promoting their lysosomal degradation and inhibiting HBV expression and replication. Our findings show a parent compound as potential anti-HBV agent by novel inhibitory mechanisms. Its structural and functional optimization need be further explored for development of novel anti-HBV agents.

Author Contributions: Conceptualization，H.A., S.M. and C.L.; Formal Analysis, Lanlan Liu, Lulu Liu, F.C., and H.W.; investigation, Lanlan Liu, Lulu Liu, and H.W.; writing—original draft preparation, H.W, C.L. and S.M.; writing—review and editing, H.W, C.L., H.A. and S.M.; supervision, project administration, and funding acquisition, S.M. All authors have read and agreed to the published version of the manuscript.

Funding: This work was funded by a grant from National Key R&D Program of China (2022YFC2304203), the Industrial innovation team grant from Foshan Industrial Technology Research Institute (2018HS), and grants from the National Natural Science Foundation of China (32070163), Foshan High-level Hospital construction DengFeng plan, and Guangdong Province biomedical innovation platform construction project tumor immunotherapy.

Data Availability Statement: All data are available in the main text or the Supplementary Materials.

Conflicts of Interest: The authors declare no conflicts of interests.

Reference

1. Seeger, C.; Mason, W.S. Molecular Biology of Hepatitis B Virus Infection. *Virology* **2015**, *479–480*, 672–686, doi:10.1016/j.virol.2015.02.031.
2. Tsukuda, S.; Watashi, K. Hepatitis B Virus Biology and Life Cycle. *Antiviral Res* **2020**, *182*, 104925, doi:10.1016/j.antiviral.2020.104925.
3. Cornberg, M.; Wong, V.W.-S.; Locarnini, S.; Brunetto, M.; Janssen, H.L.A.; Chan, H.L.-Y. The Role of Quantitative Hepatitis B Surface Antigen Revisited. *J Hepatol* **2017**, *66*, 398–411, doi:10.1016/j.jhep.2016.08.009.
4. Lan, P.; Zhang, C.; Han, Q.; Zhang, J.; Tian, Z. Therapeutic Recovery of Hepatitis B Virus (HBV)-Induced Hepatocyte-Intrinsic Immune Defect Reverses Systemic Adaptive Immune Tolerance. *Hepatology* **2013**, *58*, 73–85, doi:10.1002/hep.26339.
5. van der Molen, R.G.; Sprengers, D.; Binda, R.S.; de Jong, E.C.; Niesters, H.G.M.; Kusters, J.G.; Kwekkeboom, J.; Janssen, H.L.A. Functional Impairment of Myeloid and Plasmacytoid Dendritic Cells of Patients with Chronic Hepatitis B. *Hepatology* **2004**, *40*, 738–746, doi:10.1002/hep.20366.
6. Kondo, Y.; Ninomiya, M.; Kakazu, E.; Kimura, O.; Shimosegawa, T. Hepatitis B Surface Antigen Could Contribute to the Immunopathogenesis of Hepatitis B Virus Infection. *ISRN Gastroenterol* **2013**, *2013*, 935295, doi:10.1155/2013/935295.
7. Mak, L.-Y.; Seto, W.-K.; Hui, R.W.-H.; Fung, J.; Wong, D.K.-H.; Lai, C.-L.; Yuen, M.-F. Fibrosis Evolution in Chronic Hepatitis B e Antigen-Negative Patients across a 10-Year Interval. *J Viral Hepat* **2019**, *26*, 818–827, doi:10.1111/jvh.13095.
8. Cornberg, M.; Lok, A.S.-F.; Terrault, N.A.; Zoulim, F.; 2019 EASL-AASLD HBV Treatment Endpoints Conference Faculty Guidance for Design and Endpoints of Clinical Trials in Chronic Hepatitis B - Report from the 2019 EASL-AASLD HBV Treatment Endpoints Conference‡. *J Hepatol* **2020**, *72*, 539–557, doi:10.1016/j.jhep.2019.11.003.
9. Tout, I.; Loureiro, D.; Mansouri, A.; Soumelis, V.; Boyer, N.; Asselah, T. Hepatitis B Surface Antigen Seroclearance: Immune Mechanisms, Clinical Impact, Importance for Drug Development. *J Hepatol* **2020**, *73*, 409–422, doi:10.1016/j.jhep.2020.04.013.
10. Bazinet, M.; Pântea, V.; Cebotarescu, V.; Cojuhari, L.; Jimbei, P.; Albrecht, J.; Schmid, P.; Le Gal, F.; Gordien, E.; Krawczyk, A.; et al. Safety and Efficacy of REP 2139 and Pegylated Interferon Alfa-2a for Treatment-Naive Patients with Chronic Hepatitis B Virus and Hepatitis D Virus Co-Infection (REP 301 and REP 301-LTF): A Non-Randomised, Open-Label, Phase 2 Trial. *Lancet Gastroenterol Hepatol* **2017**, *2*, 877–889, doi:10.1016/S2468-1253(17)30288-1.
11. Hui, R.W.-H.; Mak, L.-Y.; Seto, W.-K.; Yuen, M.-F. RNA Interference as a Novel Treatment Strategy for Chronic Hepatitis B Infection. *Clin Mol Hepatol* **2022**, *28*, 408–424, doi:10.3350/cmh.2022.0012.
12. Kim, S.W.; Yoon, J.S.; Lee, M.; Cho, Y. Toward a Complete Cure for Chronic Hepatitis B: Novel Therapeutic Targets for Hepatitis B Virus. *Clin Mol Hepatol* **2022**, *28*, 17–30, doi:10.3350/cmh.2021.0093.
13. Sirafil; Askar; Ilhamjan; Xawkat; Halmurat Regulation of P53, Fas and Bcl-2 Gene Expressions with Artemisia Flavonoid in Human Hepatoma. *Chin J Biochem Mol Biol* **2001**, *17*, 226–229, doi:10.13865/j.cnki.cjbmb.2001.02.020.
14. Fang, M.; Chao, Q.; Lan, Y.; Liu, X.; Xu, X.; Fan, Y. Antibacterial Effect of the Extract from Artemisia Rupestris L. *Food Science and Technology* **2010**, *36*, 160–162, doi:10.13684/j.cnki.spkj.2011.01.071.
15. Zhao, J.; Aisa, H.A. Synthesis and Anti-Influenza Activity of Aminoalkyl Rupestonates. *Bioorg Med Chem Lett* **2012**, *22*, 2321–2325, doi:10.1016/j.bmcl.2012.01.056.
16. Ma, L.-L.; Wang, H.-Q.; Wu, P.; Hu, J.; Yin, J.-Q.; Wu, S.; Ge, M.; Sun, W.-F.; Zhao, J.-Y.; Aisa, H.A.; et al. Rupestonic Acid Derivative YZH-106 Suppresses Influenza Virus Replication by Activation of Heme Oxygenase-1-Mediated Interferon Response. *Free Radic Biol Med* **2016**, *96*, 347–361, doi:10.1016/j.freeradbiomed.2016.04.021.
17. Li, C.; Wang, Y.; Wang, S.; Wu, B.; Hao, J.; Fan, H.; Ju, Y.; Ding, Y.; Chen, L.; Chu, X.; et al. Hepatitis B Virus mRNA-Mediated miR-122 Inhibition Upregulates PTTG1-Binding Protein, Which Promotes Hepatocellular Carcinoma Tumor Growth and Cell Invasion. *J Virol* **2013**, *87*, 2193–2205, doi:10.1128/JVI.02831-12.
18. Schinazi, R.F.; Ehteshami, M.; Bassit, L.; Asselah, T. Towards HBV Curative Therapies. *Liver Int* **2018**, *38 Suppl 1*, 102–114, doi:10.1111/liv.13656.
19. Fisicaro, P.; Barili, V.; Rossi, M.; Montali, I.; Vecchi, A.; Acerbi, G.; Laccabue, D.; Zecca, A.; Penna, A.; Missale, G.; et al. Pathogenetic Mechanisms of T Cell Dysfunction in Chronic HBV Infection and Related Therapeutic Approaches. *Front Immunol* **2020**, *11*, 849, doi:10.3389/fimmu.2020.00849.
20. Yuen, M.-F.; Chen, D.-S.; Dusheiko, G.M.; Janssen, H.L.A.; Lau, D.T.Y.; Locarnini, S.A.; Peters, M.G.; Lai, C.-L. Hepatitis B Virus Infection. *Nat Rev Dis Primers* **2018**, *4*, 18035, doi:10.1038/nrdp.2018.35.
21. Ahn, S.H.; Park, Y.N.; Park, J.Y.; Chang, H.-Y.; Lee, J.M.; Shin, J.E.; Han, K.-H.; Park, C.; Moon, Y.M.; Chon, C.Y. Long-Term Clinical and Histological Outcomes in Patients with Spontaneous Hepatitis B Surface Antigen Seroclearance. *J Hepatol* **2005**, *42*, 188–194, doi:10.1016/j.jhep.2004.10.026.

22. Lee, H.W.; Lee, J.S.; Ahn, S.H. Hepatitis B Virus Cure: Targets and Future Therapies. *Int J Mol Sci* **2020**, *22*, 213, doi:10.3390/ijms22010213.
23. Jiang, B.; Hildt, E. Intracellular Trafficking of HBV Particles. *Cells* **2020**, *9*, 2023, doi:10.3390/cells9092023.
24. Nayagam, J.S.; Cargill, Z.C.; Agarwal, K. The Role of RNA Interference in Functional Cure Strategies for Chronic Hepatitis B. *Curr Hepatology Rep* **2020**, *19*, 362–369, doi:10.1007/s11901-020-00548-4.
25. Yeo, Y.H.; Ho, H.J.; Yang, H.-I.; Tseng, T.-C.; Hosaka, T.; Trinh, H.N.; Kwak, M.-S.; Park, Y.M.; Fung, J.Y.Y.; Buti, M.; et al. Factors Associated With Rates of HBsAg Seroclearance in Adults With Chronic HBV Infection: A Systematic Review and Meta-Analysis. *Gastroenterology* **2019**, *156*, 635-646.e9, doi:10.1053/j.gastro.2018.10.027.
26. Yuen, M.-F.; Locarnini, S.; Given, B.; Schluep, T.; Hamilton, J.; Kalmeijer, R.; Beumont, M.; Lenz, O.; Cloherty, G.; Jackson, K.; et al. First Clinical Experience with RNA Interference-Based Triple Combination Therapy in Chronic Hepatitis B: JNJ-3989, JNJ-6379 and a Nucleos(t)Ide Analogue.; Boston, MA, USA, November 8 2019.
27. Gerken, G.; Manns, M.; Gerlich, W.H.; Hess, G.; Meyer zum Büschenfelde, K.H. Pre-S Encoded Surface Proteins in Relation to the Major Viral Surface Antigen in Acute Hepatitis B Virus Infection. *Gastroenterology* **1987**, *92*, 1864–1868, doi:10.1016/0016-5085(87)90617-2.
28. Bruss, V.; Vieluf, K. Functions of the Internal Pre-S Domain of the Large Surface Protein in Hepatitis B Virus Particle Morphogenesis. *J Virol* **1995**, *69*, 6652–6657, doi:10.1128/JVI.69.11.6652-6657.1995.
29. Garcia, T.; Li, J.; Sureau, C.; Ito, K.; Qin, Y.; Wands, J.; Tong, S. Drastic Reduction in the Production of Subviral Particles Does Not Impair Hepatitis B Virus Virion Secretion. *J Virol* **2009**, *83*, 11152–11165, doi:10.1128/JVI.00905-09.
30. Pfefferkorn, M.; Schott, T.; Böhm, S.; Deichsel, D.; Felkel, C.; Gerlich, W.H.; Glebe, D.; Wat, C.; Pavlovic, V.; Heyne, R.; et al. Composition of HBsAg Is Predictive of HBsAg Loss during Treatment in Patients with HBeAg-Positive Chronic Hepatitis B. *J Hepatol* **2021**, *74*, 283–292, doi:10.1016/j.jhep.2020.08.039.
31. Dikic, I. Proteasomal and Autophagic Degradation Systems. *Annu Rev Biochem* **2017**, *86*, 193–224, doi:10.1146/annurev-biochem-061516-044908.
32. Yamamoto, H.; Matsui, T. Molecular Mechanisms of Macroautophagy, Microautophagy, and Chaperone-Mediated Autophagy. *J Nippon Med Sch* **2024**, *91*, 2–9, doi:10.1272/jnms.JNMS.2024_91-102.
33. Yang, J.Y.; Wu, Y.-H.; Pan, M.Y.-C.; Chiou, Y.-T.; Lee, R.K.-L.; Li, T.-N.; Wang, L.H.-C. Chemical-Induced Degradation of PreS2 Mutant Surface Antigen via the Induction of Microautophagy. *Antiviral Res* **2022**, *207*, 105417, doi:10.1016/j.antiviral.2022.105417.